Non-Linear Behaviour of Masonry under Tension

Rob van der Pluijm
Eindhoven University of Technology, Faculty of Architecture, Building and Planning
TNO Building and Construction Research

For the micro-modelling of masonry in numerical programs that take non-linear behaviour into account, a complete description of the behaviour of masonry components has to be available. "Complete" means that, apart from the initial stiffness and the strength, the behaviour beyond the peak in the σ-ε diagram is described.
This article gives an overview of deformation controlled tensile and flexural tests that have been carried out since 1990 by the author to establish the behaviour prior and beyond the maximum load under tension. All tests were carried under a monotonic increase of a deformation measured on the specimen itself.
The behaviour of units and mortar-joints under tension showed a great similarity to that of concrete. Experience in describing the non-linear behaviour of concrete under tension could be applied to the masonry components. The mode I fracture energy of units is of the same magnitude as that of concrete. The mode I fracture energy of mortar-joints is approximately one order of magnitude smaller and showed a great scatter.

Key words: **units, mortar-joints, (post peak) behaviour, mode I fracture energy, deformation controlled tests**

1 Introduction

Masonry design rules and calculation methods are mainly of traditional and empirical nature, reflecting national or regional building traditions. The great variety of units and mortars in different countries also contributes to a phenomenological approach that gives solutions for a relatively small range of products and applications. To be able to rationalise the design of masonry, fundamental insight in the behaviour has to be available. Nowadays combined numerical and experimental research tools are essential to gain insight in the fundamental behaviour and eventually making possible the rationalisation of design rules. The main goal of the experiments outlined in this article was to find a description of the behaviour of the masonry components under tension, making the numerical modelling of masonry possible on a meso-level. For a complete description on the meso-level, also the non-linear behaviour of mortar-joints under combined shear and normal stresses has to be known (see Van der Pluijm, 1993). Modelling of masonry on a meso-level implies the modelling of units and mortar-joints with different elements and if necessary with different constitutive

HERON, Vol. 42, No. 1 (1997) ISSN 0046-7316

models. For detailed information on the numerical modelling of masonry, the reader is referred to Lourenço et al.(1995).

Before describing the tensile and flexural tests and discussing their results, the units and mortar used will be characterised. The materials chosen were based on Dutch building practice.

2 Materials

2.1 *Introduction*

Clay bricks, calcium silicate bricks[1], blocks[2] and elements[3] and normal density concrete brick were used separately and in combination with different types of mortars.
In 1990, the first series of tensile tests were performed with yellow wire cut clay bricks (brand Joosten), red soft mud clay bricks (brand Vijf Eiken) and calcium silicate bricks separately and in combination with two mortar compositions: 1:2:9 and 1:½:4½ (cement:lime:sand ratio by volume). With these combinations a wide variety of strength classes was covered.
In the series performed in 1993 also tensile tests were carried out with parts of calcium silicate elements and concrete bricks and a very strong wire cut clay brick, in combination with factory made general purpose mortars designed for that type of bricks. These tests included specimens with thin layer joints.
In the tensile and flexural tests that were carried out in 1995, a new soft mud clay brick (brand Rijswaard) was used, because the previously used soft mud clay brick was no longer available on the market. Also the yellow wire cut clay brick, parts of calcium silicate blocks and the normal density concrete block were used.

2.2 *Units*

In Table 1, some physical characteristics of all units are presented. The values were determined using the appropriate Dutch standards as indicated in the table. The normalized compressive strength values $f^{u}_{c;normalized}$ were calculated using the values determined according to the Dutch standards with the conversion table of prEN 772-1:1995. This conversion is intended to give a strength value for the unit with a normalized height of 100 mm.

---

[1] In this paper the term brick is used for units with maximum dimensions of approx. $214 \times 102 \times 90$ mm^3

[2] The term block is used for units with dimensions greater than bricks but not greater than approx. $500 \times 250 \times 250$ mm^3

[3] The term elements is used for units with dimensions $900 \times (100 - 300) \times 600$ mm^3

Table 1. Overview of units and their properties.

unit type	manufacturer	code	dimensions [mm³]	free water absorption 48h [mass-%]	mass by volume (dry) [kg/m³]	mean compressive strength		
						method	f_c^u [N/mm²]	$f_{c;normalized}^u$ [N/mm²]
wire cut clay brick	Joosten Wessen	wc-JO	204×98×50	7.3	1900	NEN 2498	66	50
soft mud clay brick	Vijf Eiken	sm-VE	208×98×50	17.4	1610	NEN 2498	33	25
soft mud clay brick	Rijswaard	sm-RIJ	206×96×50	15.5	1630	NEN 2498	27	20
high strength wire cut clay brick	Joosten Kessel	hswc-JOK	206×98×50	-	-	NEN 2498	81	67
calcium silicate brick	Loevestein	CS-brick	212×100×53	11.5	1880	NEN 3836	40	30
calcium silicate block	Loevestein	CS-block	439×100×198	12.0	2010	NEN 3836	30	41
calcium silicate element	Loevestein	CS-el	900×100×600	-	-	-	15*	15*
normal density concrete brick	MBI smooth facing brick	MBI	207×100×50	-	2370	NEN 7027	70	53

* not tested, strength according to the manufacturer

2.3 *Constituents of laboratory made mortars*

The grading analyses of the sands for the different mortars are presented in Figure 1. The sieve sizes are indicated along the horizontal axis.

Two types of lime were used:
- hydrated shell lime
- hydrated lime with an air-entrainer (brand Mekal)

The cement used was always ordinary Portland cement type A (brand ENCI). Since 1995 this cement is sold as CEM I 32.5 R. The compressive strength of these cements is at least 32.5 N/mm² after 28 days according to NEN 3550:1995. It is determined with a specimen which has the same dimensions as a mortar specimen (see section 2.5).

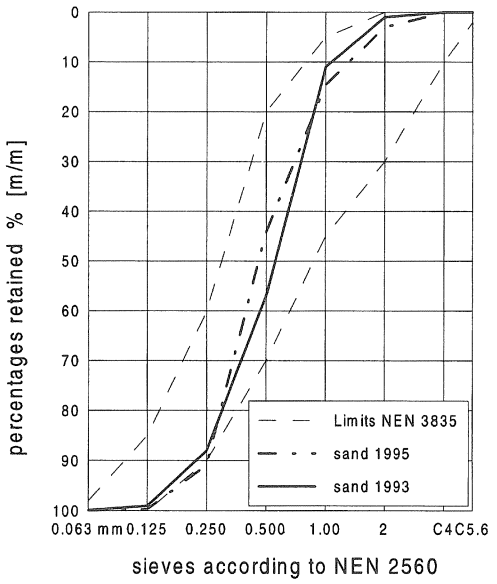

Fig. 1. Grading analyses of sands.

2.4 *Mortar preparation*

The laboratory made mortar composition was specified by volume, but weighed batches were used. The ratios by volume of the mortar were converted to ratios by mass using the following bulk densities:

cement: 1250 kg/m^3

lime: 600 kg/m^3

dry sand: 1400 kg/m^3

The amount of water was based on the workability of the mortar. The target value for the flow was 175 ± 10 mm according to NEN 3835:1991.

The dry constituents were mixed during approximately 3 minutes before the water was added. Next the mortar was mixed during 3–5 minutes before determining the flow and in case of an addition of water mixed again during a few minutes.

Factory made mortars were prepared according to the prescriptions of the manufacturers.

2.5 *Mortar properties*

Over the years, many different mortar batches were used. The mean compressive strength value in a test series according to the Dutch standard NEN 3835:1991 is presented Table 2. The Dutch standard prescribes a prism 40 × 40 × 160 mm^3 that is first used in a 3-point bending test. Next the compressive strength is determined on six halve prisms that remain from the flexural tests.

The value obtained is comparable with a test on a 40 mm mortar cube.

Table 2. Overview of the average mortar compressive strength fmortarc according to NEN 3835: 1991 by test-series and by unit type.

test-series	mortar (composition by volume parts c:1: s if appropriate)	used with units	mortar-joint thickness [mm]	f_c^{mortar} at 28 d. [N/mm²]
tensile test 1990	gpm 1:1:6 (shell lime)	CS-brick	14	8.2
	gpm 1:2:9 (shell lime)	wc-JO, sm-VE, CS-brick	14	3.0
	gpm 1:½:4½ (shell lime)	wc-JO sm-VE	14	17.6
tensile tests 1993	fmgpm (Beamix 312)	MBI-concrete brick	14	11.6
	tlm for clay bricks (Ytong)	hswc-JOK	3	32.7
tensile and bending tests 1995	gpm 1:1:6 (lime with air entrainer)	CS-brick, wc-JO, sm-RIJ	12.5	8.1
	tlm (Calsifix)	CS-block	2	19.9
	fmgpm (Beamix C 312)	MBI	12.5	16.7
	tlm for concrete bricks (Beamix C62)	MBI	3	25.0
tlm:	thin layer mortar (always factory made):			
gpm:	general purpose mortar (traditional joint thickness, dense aggregate):			
fmgpm:	factory made general purpose mortar:			

2.6 *Fabrication of Specimens*

Throughout the years, different pretreatements of units and curing regimes were followed. In 1990 most bricks were pre-wetted. The soft mud clay bricks were always pre-wetted resulting in a suction rate of approximately 1.1 kg/m²/min for the sm-VE clay bricks in 1990 and 1.4 kg/m²/min for the sm-RIJ clay bricks in 1995. In 1990 the wire cut clay brick (wc-JO) was prewetted resulting in a suction rate 0.5-0.7 kg/m²/min. In 1995 this clay brick was used directly from the stock in the laboratory (IRA = 1.9 kg/m²/min). This was also the case with the high strength wire cut clay brick hswc-JOK (suction and water absorption properties were not determined). The concrete bricks were always used right away (laboratory dry condition). The calcium silicate bricks in 1990 were pre-wetted until a moisture content of 5.5-6.5% was reached. The bond faces of the parts of the CS-blocks used in 1995, were prewetted with a brush just before laying. The last procedure is an accordance with the instructions of the Dutch calcium silicate industry when blocks are processed with thin layer mortar.

All specimens in 1990 were cured during three days by close covering them with plastic bags in a 20°C-95% RH climate-room. Subsequently, they were placed in 20°C-60% RH. In 1993 and 1995 the specimens were cured during 7 days in plastic and than left undisturbed in 20°C-60% RH, except for the specimens made with calcium silicate blocks with thin layer mortar. These specimens were not covered with plastic in order to simulate practical conditions for these blocks.

3 Tensile Tests

3.1 *Testing Arrangement*

For the series performed in 1990 and 1993 a testing arrangement of the Stevin Laboratory of the Delft University of Technology was used (see Figure 2). For the series of 1995 a newly developed arrangement in the Pieter van Musschenbroek Laboratory of the Eindhoven University of Technology was used (see Figure 3). In both arrangements it is intended to provide a an as good as possible full restraint against rotation of the platens between which the specimens are glued. In the arrangement of Delft this is done by connecting the top platen to a stiff guiding system in such a way that it can only move vertically where in Eindhoven the top platen is part of a parallelogram disabling a possibility of rotation. It is realised that a full restraint can only be approximated and that the rotational stiffness of the specimen itself also plays a role in deformation controlled tests. As a result non-uniform crack-opening occurs, resulting in a typical S-shape of the descending branch as will be discussed later on (see also Hordijk, 1992).

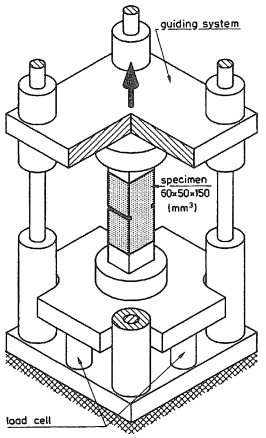

Fig. 2. Tensile Testing Arrangement of the Stevin Laboratory (Hordijk, 1992).

In the testing arrangement of the Stevin Laboratory the load is measured under the bottom platen, so the friction between the guiding system and the top platen has no influence on the measured force.

In the test set-up of the Pieter van Musschenbroek laboratory the spring-forces in the arms and dead weight of the "red box" (a red painted steel member with a rectangular hollow section $300 \times 300 \times 10$ mm), have to be subtracted from the measured load. These loads are determined using the internal linear variable differential transducer (LVDT) of the actuator in combination with a force-displacement diagram established without a specimen.

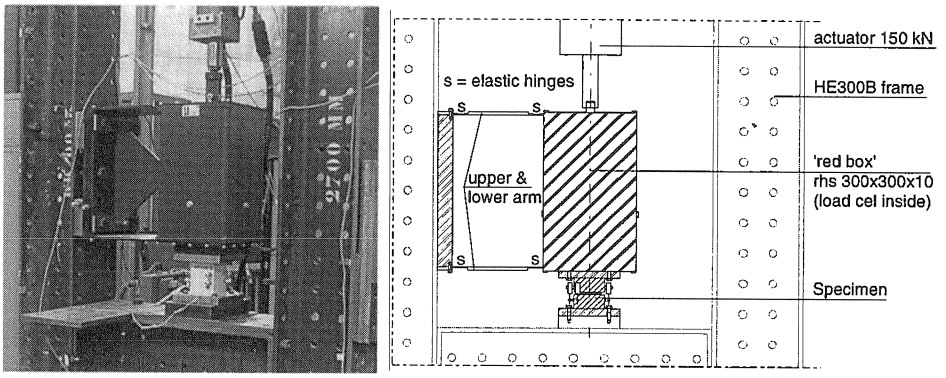

Fig. 3. Tensile Testing Arrangement of the Pieter van Musschenbroek Laboratory.

In both arrangements LVDTs are glued on the specimens (see Figure 4). These LVDTs are used to control the increase of the deformation over a crack that will develop during the test. The gauge length must include a weak cross section of the specimen to fix the location of the crack. In case of a masonry specimen the joint is a natural weak cross section, but in case of testing units, the weak cross section is created by reducing a cross section within the gauge length by a symmetric saw cut. The testing arrangement makes it possible to establish a stress-crack width relation that approaches the real material behaviour and the mode I fracture energy G_{fI} of a specimen. In Van Mier et al. (1994) the influence of the boundary conditions of the testing arrangement on the fracture energy is discussed in detail.
The gauge length used in the Stevin laboratory varied between 25 and 35 mm. The gauge length used in the Pieter van Musschenbroek laboratory was always 30 mm.

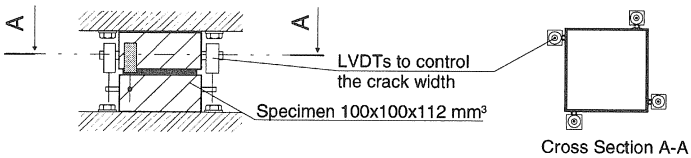

Fig. 4. Location of LVDTs used to control the increase of deformation during a test.

For a comprehensive description of the testing technique applied in the Stevin laboratory, the reader is referred to Hordijk (1992).

3.2 *Specimens*

Specimens made out of units and masonry specimens were used. They are shown in Figure 5.

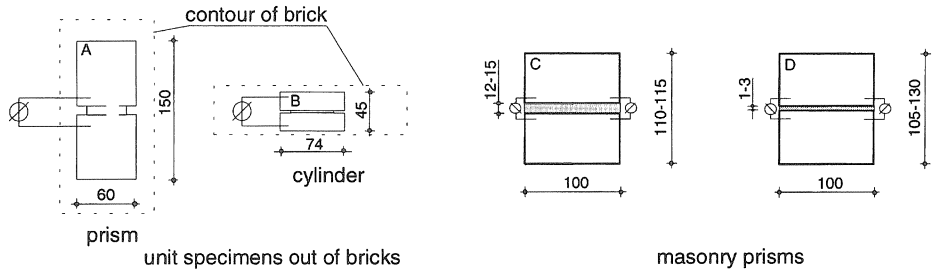

Fig. 5. Tensile specimens.

The exact dimensions of the masonry specimens depended on the unit type used. The unit specimens were sawn out of a unit using a water cooled diamond saw or a hollow diamond drill. They were dried for 48 hours at 50 °C and subsequently left with the masonry specimens. In 1990 the age at time of testing was at least three months. This long period was chosen to exclude changes in strength of the masonry specimens during testing, because it was expected that testing could take a relatively long time. Later on, the bond strength development in the laboratory was established and it was concluded that the increase of strength after 28 days is very moderate (see Vermeltfoort et al., 1995) and it was decided that testing could start at 28 days.
The bats for the masonry specimens were made by sawing bricks in half. When blocks were used the "bats" were sawn out of blocks in such a way that the original bond surfaces were preserved (see Figure 6).

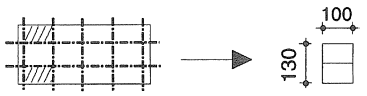

Fig. 6. Sawing of blocks.

3.3 *Results and discussion*

If a tensile test is controlled beyond the maximum load, a curved diagram as presented in Figure 7 can be obtained.

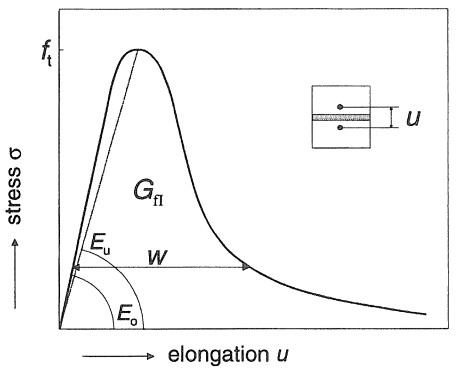

Fig. 7. Schematic diagram of a deformation (u) controlled tensile test.

The area under the curved diagram of Figure 7 is definied as the mode I fracture energy G_{fI}.
The fracture energy is the amount of energy by unit of area that is needed to create a crack in which no tensile stresses can be transferred.
The tensile strength f_t was calculated from:

$$f_t = \frac{F_u}{A} \tag{1}$$

in which:
F_u is the ultimate force;
A is the cross sectional area of the specimen where the crack has occurred.
To be able to calculate the deformation of the mortar-joint in the masonry specimens, the measurements had to be corrected for the elastic deformation in the part of the unit within the gauge length. This was done using stiffness values for the units determined in accompanying compressive or tensile tests. These stiffness values for the units are presented in Table 3. They were determined with linear regression in the first, almost linear part of the σ-ε diagram.

Table 3. Modulus of elasticity E^u [N/mm^2] of units.

unit type	compression	tension
wc-JO	16700 (1990)	16605 (1995)
sm-VE brick	6050 (1990)	-
hswc-JOK	9900 (1993)	-
CS-brick	13400 (1990)	-
CS-block	12190 (1993)	12805 (1995)
MBI	17000 (1993)	-

With the calculated deformations of the mortar-joints, stiffness values could be established.
The initial stiffness E_o and the secant modulus E_u of the masonry specimens and mortar-joints were calculated (see Figure 7). The initial stiffness was calculated with linear regression using the data up to a variable load level. This load level was established by calculating the correlation coefficient r for levels between $0.5 f_t$ and $0.9 f_t$ at intervals of $0.05 f_t$. Finally the level with the maximum value of r was selected. The mean level of r by series is presented in the tables in the annex.
Stiffness values of the unit specimens are not presented because their cross section was locally reduced by the saw cuts, so the cross section within the gauge length was not constant resulting into ambiguous, 20-40% lower values compared with those in Table 3, when the area of the reduced cross section was used to calculate the stiffness.
When the mortar-joint thickness is small and the stiffness of the specimen within the gauge length does not differ much from the unit stiffness, the outcome of the calculated stiffness of the mortar-joint becomes highly sensitive for the stiffness of the unit used and the thickness of the joint, which is not easy to measure when it becomes thinner and thinner. The modulus of elasticity of the

mortar-joint was calculated assuming that the Poisson's ratios of both units and mortar were equal. Then it can be derived that:

$$E^{j} = \frac{t^{j} E^{j+u} E^{u}}{E^{u}(t^{u} + t^{j}) - E^{j+u} t^{u}} \tag{2}$$

in which:

E^{j} is the modulus of elasticity of the joint;

E^{u} is the modulus of elasticity of the unit;

t^{u} is the thickness of the joint;

t^{u} is the thickness of parts of the units within the gauge length;

E^{j+u} is the modulus of elasticity of the specimen within the gauge length, following directly from the measurements.

In Figure 8 the influence of:

- relatively small changes of the value used for the stiffness of the unit,
- a small change of the measured deformation (via E^{j+u}) and
- the joint thickness

on the calculated stiffness of the joint, is demonstrated.

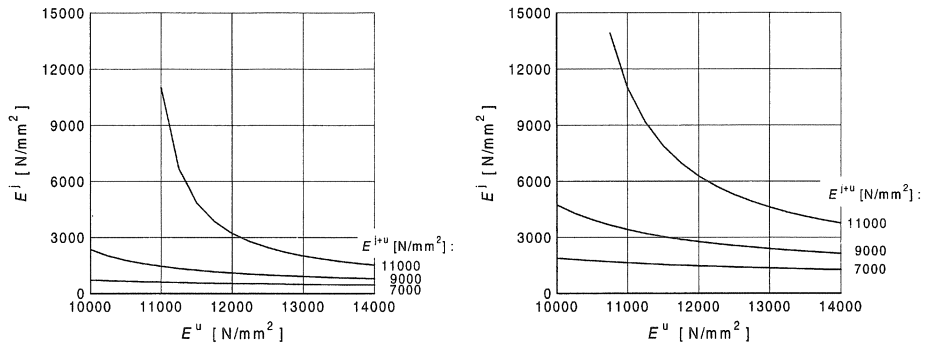

(a) t^{j} = 1 mm; t^{u} = 29 mm *(b) t^{j} = 3 mm; t^{u} = 27 mm*

Fig. 8. Average stiffness of thin layer mortar joint as a function of the unit stiffness E^{u} and measured stiffness E^{j+u}.

Consequently, the calculated stiffness of especially thin layer joints was unreliable in some cases. In these cases the stiffness of the specimen within the gauge length has been presented. This modulus of elasticity is indicated as E^{j+u}.

In Van der Pluijm et al. (1991) is was shown that the descending branch of masonry under tension (for both units and bonding surface) can be described with a formula developed by Hordijk and Reinhardt for plain concrete (see Hordijk, 1992):

$$\frac{\sigma}{f_t} = \left(1 + \left(c_1 \frac{w}{w_c}\right)^3\right) e^{-c_2 \frac{w}{w_c}} - \frac{w}{w_c}(1 + c_1^3) e^{-c_2} \qquad (3)$$

in which :

σ is the tensile stress;

f_t is the tensile (bond)strength;

c_1, c_2 are dimensionless constants, respectively 3.0 en 6.93;

w is the crack width (see Figure 7);

w_c is the crack width at which no stresses are being transferred any more: $w_c \approx 5.14 \frac{G_{fI}}{f_t}$;

G_{fI} is the mode I fracture energy.

An alternative formulation has been used by Lourenço et al. (1996):

$$\frac{\sigma}{f_t} = e^{-\frac{f_t}{G_{fI}} w} \qquad (4)$$

Both expressions give nearly the same result. Eq. (4) is less steep in the first part of the descending branch. Their applicability will be demonstrated later.

The results of all tests are presented in tables in the annex. In each table, test results for one type of unit have been presented. The average results are also presented in Table 4. In this table the coefficient of variation (CV) is given between brackets, but it is emphasised that its reliability based on a few individual test results is very small. The reader is referred to the annex for the exact amount of tests in each series. Only the larger series with wc-JO clay bricks + 1:1:6 mortar and the CS-block masonry with thin layer mortar consisted of enough specimens to determine a more reliable CV. However, the scatter within these series is of the same magnitude as of the other series. For the wc-JO clay bricks with 1:1:6 mortar this is not strange, because this series was divided in six sub-series with different mortar batches (see also Table 8). The CV within the sub-series are also large for the tensile strength (25-35%). The series with CS-block masonry with thin layer mortar consisted of three sub-series. By sub-series (12 tests) the CV of the tensile strength varied between 21% and 27%. It may be concluded that the CV's found in the small series are not influenced much by the sample size. In general CV's of 20% to 30% are typical for bond strength tests (see De Vekey et al., 1994).

Table 4. Average results of tensile tests.

specimen type (see Figure 5)	mortar	E_o^j [N/mm^2]	E_u^j [N/mm^2]	G_{fl} [N/m]	f_t [N/mm^2]
sm-VE prism	-	-	-	61 (24%)	2.47 (14%)
sm-VE cylinder	-	-	-	73 (3%)	1.50 (4%)
wc-JO prism	-	-	-	117 (-)	2.36 (21%)
wc-JO cylinder	-	-	-	128 (3%)	3.51 (3%)
CS brick prism	-	-	-	67 (17%)	2.34 (10%)
CS element prism	-	-	-	47 (-)	1.17 (49%)
sm-VE masonry	1:2:9	610 (12%)	470 (12%)	7.8 (65%)	0.22 (60%)
	1:½:4½	670 (69%)	320 (76%)	4.2 (32%)	0.13 (101%)
wc-JO masonry	1:2:9	2900 (13%)	1410 (52%)	11.5 (64%)	0.30 (24%)
	1:1:6	2370 (55%)	1220 (57%)	5.5 (70%)	0.40 (39%)
	1:½:4½	6000 (20%)	3840 (37%)	6.8 (51%)	0.50 (29%)
hswc-JOK masonry	tlm	4402 (16%)	3140 (35%)	17.1 (35%)	2.24 (26%)
CS-brick masonry	1:2:9	5110 (17%)	1490 (12%)	*	0.32 (34%)
	1:1:6	2540 (19%)	1790 (18%)	*	0.33 (51%)
CS-block masonry	tlm	7990 (54%) **	6040 (53%) **	3.3 (41%)	0.33 (27%)
MBI masonry	fmgpm	8040 (26%)	7470 (35%)	11.3 (-)	0.73 (19%)

* uncontrolled failure

** presented value of E-modulus determined over whole gauge length (30 mm) (see also Table 9)

Examples of stress-displacement curves that were obtained with specimens in the series wc-JO bricks with 1:1:6 mortar, are presented in Figure 9.

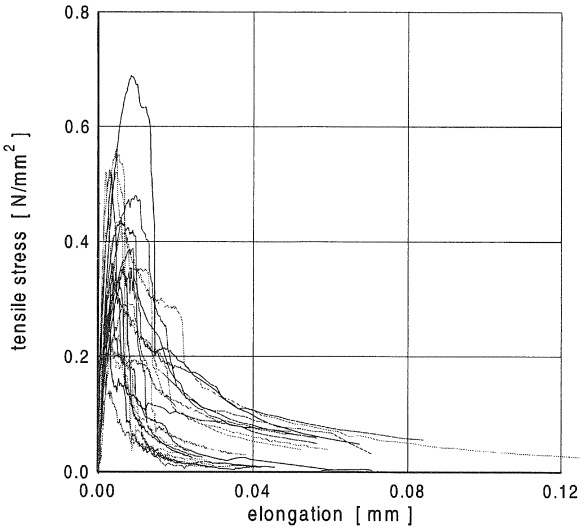

Fig. 9. Stress-displacement curves of controlled tests in series with wc-JO bricks and 1:1:6 mortar.

Although a diagram of one test can hardly be identified in Figure 9, all curves are presented together to give an impression of the scatter of the tensile bond strength and of the fracture energy (area under the curves).

Stiffness

From Table 4 it can be observed that:

- The stiffness of the mortar-joints is dependent on the type of units. The stiffness of the same mortar hardened between different units, can result in stiffness values that differ a factor 5 to 10.
- The scatter of results within a series is of the same magnitude as of the bond strength.
- It was not possible to establish meaningful values of the stiffness for the thin layer mortar joints in the series with CS-blocks and thin layer mortar for each specimen.

Using the average stiffness of the specimens of the series with CS-blocks and thin layer mortar to establish the stiffness of the mortar-joint with eq. (2), lead to the results presented in Table 5.

Table 5. Mean stiffness values E_o^j for thin layer mortar joints in CS-block masonry depending on joint thickness with $E^u = 12190$ N/mm^2, $t^u + t^j = 30$ mm.

joint thickness [mm]	E^{j+u} [N/mm^2]	
	7990	6040
1	727	386
2	1372	749
3	1948	1090

From the results it can be observed that the joint thickness and stiffness (in a numerical model) is important. It must be consistent with the data concerning t^u+t^j, E^u and E^{u+j}. To avoid inaccuracy of the joint thickness with thin layer joints, the height of each bat should be measured prior to laying and subsequently the joint thickness can be established by measuring the height of the hardened specimens.

Tensile strength

The CS unit was only tested in the direction parallel to the bed joint, because it is supposed that this unit-type shows isotropic behaviour.

In most of the masonry specimens a crack formed at the bond surface between mortar and unit. The bond surface after fracture of masonry with CS-units was remarkably smooth.

From the results in Table 4, it can be observed that:

- The wire cut Joosten clay brick is stronger in the direction perpendicular to the bed joint (WC-JO cylinder), while the soft mud Vijf Eiken brick is stronger in the direction parallel to the bed joint (SM-VE prism). This result can be explained by the difference in orientation of the layers in the clay bricks due to the fabrication process. The low CV for the tensile strength of the cylindrical specimens cannot be explained in this way.
- The tensile bond strength of SM-VE with mortar 1:2:9 (0.22 N/mm^2) is higher compared with that of SM-VE with mortar 1:½:4½ (0.13 N/mm^2). The probability for the difference in mean equals 0.19 when the hypothesis of less strength is tested with a t-test. The higher bond strength with mortar 1:2:9 is remarkable because mortar 1:½:4½ is stronger than mortar 1:2:9. This result may be caused by the (too) high moisture content of the SM-VE clay brick at time of laying in 1990.
- An increase of mortar strength had a positive influence on the masonry bond strength for the WC-JO brick (low suction rate). This was not the case for the SM-VE brick masonry and the CS-brick masonry.
- As already discussed, there is a great scatter in test results. Among other reasons this is caused by the influence of the effective bond surface. From close observation of the crack surface of the specimens, it became clear that the area where the mortar and unit were bonded together in the specimens differed from each other and was considerably smaller then the cross-sectional area. This phenomenon will be discussed later as the "net bond area". The bonding surface was established for the series in 1990, see Van der Pluijm (1992).
- The thin layer mortar especially developed for clay bricks in the series with the high strength wire cut clay brick JOK, performed extremely well. Here failure occurred also in the brick-mortar interface. The bond strength is of the same magnitude as of the prisms made out of normal strength bricks. The bond strength of the concrete brick masonry with the factory made general purpose mortar is also relatively high.
- The bond strength of the CS-brick masonry is reasonable. The bond strength of the CS-block masonry with the thin layer mortar is somewhat low (0.32 N/mm^2) compared with the requirements of the Dutch standards (0.4 N/mm^2), but it is a reasonable value if the moisture content of the blocks at time of laying (2–3%) and the "no-curing" regime are considered.

In Figure 10 the modulus of elasticity E_o^j of the mortar-joint in clay brick masonry with general purpose mortar is plotted against the tensile bond strength.

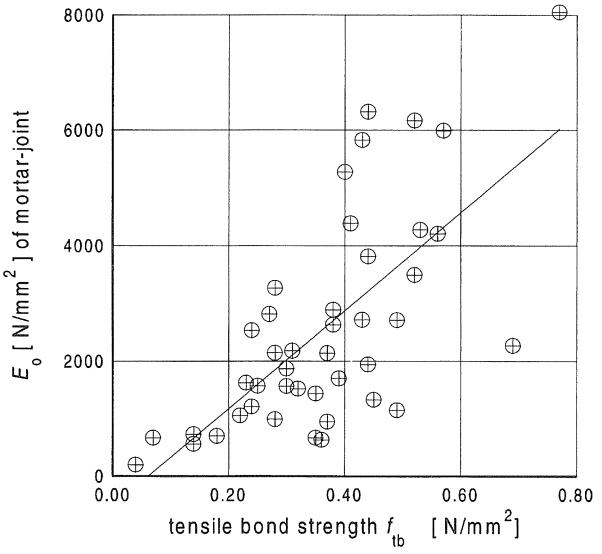

Fig. 10. Tensile bond strength versus E_o^j of the mortar-joint for clay brickwork with general purpose mortar.

A weak correlation can be observed between the tensile bond strength and E_o^j. The correlation coefficient r of the plotted linear best fit ($E_o^j = 8490 \cdot f_{tb} - 520$) equals 0.68.

Fracture energy

In 1990, all masonry specimens with CS-bricks failed uncontrolled after the ultimate load was reached. Therefore no values for the fracture energy are given. Uncontrolled failure does not mean that the fracture energy is zero as will be shown with the results of the flexural tests.

From the values for the mode I fracture energy G_{fl} in Table 4, the following can be observed:

- The fracture energy of the units is approximately one order of magnitude greater than that of the bond surface. As expected for the mortar-joints, the fracture energy is very low.
- The scatter of the mode I fracture energy of the masonry bond interface is larger than the scatter of the tensile bond strength.

If the shapes of the descending branches of the units and the masonry specimens are equal (which is the case), the brittleness of materials can be compared using the characteristic length l_{ch} defined by Petersson, (1981):

$$l_{ch} = \frac{G_{fl} \cdot E}{f_t^2} \tag{5}$$

in which:

G_{fl} is the fracture energy;

E is the modulus of elasticity;

f_t is the tensile (bond) strength.

With an increase of l_{ch}, the brittleness decreases. When eq. (5) is used to compare the brittleness of the units and the masonry bond interface, the difference is limited.

In Figure 11 the fracture energy is plotted against the tensile bond strength for all clay brick specimen with general purpose mortar and for the CS-block specimen with thin layer mortar.

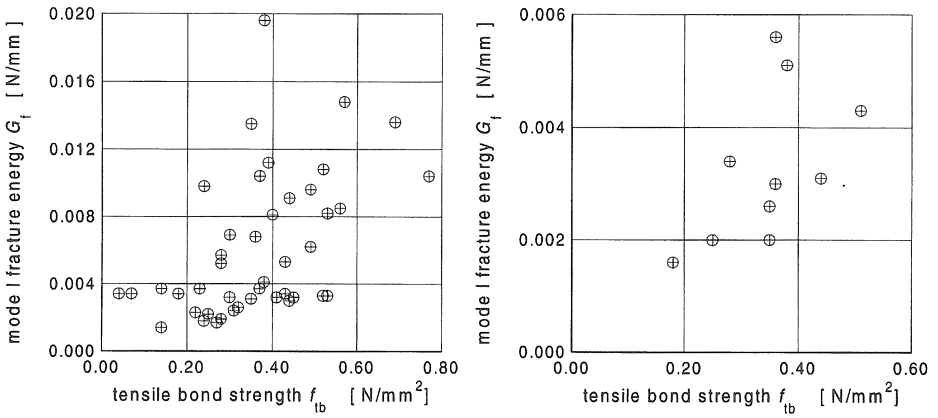

Fig. 11. Tensile bond strength versus mode I fracture energy for a) clay brick masonry with general purpose mortar and b) calcium silicate masonry with thin layer mortar.

It can be observed that there is no clear correlation between both parameters, but with an increasing bond strength, the fracture energy also tends to increase.
An example of the prediction of the descending branches with equations (3) and (4) is given in Figure 12.

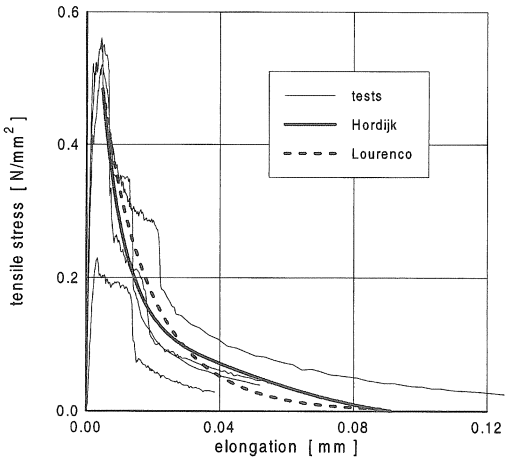

Fig. 12. Stress-displacement curves of the last sub-series with WC-JO clay bricks and 1:1:6 mortar (see Table 8), including the average theoretical descending branches according Hordijk – eq. (3) and Lourenço – eq. (4).

The typical S-shape in the descending branches of the stress-crack width diagrams of the tests is caused by the non-uniform opening of the crack (see Hordijk, 1992). The non-uniform opening is demonstrated in Figure 13, showing the displacements measured with the 4 LVDTS at the corners of the specimen.

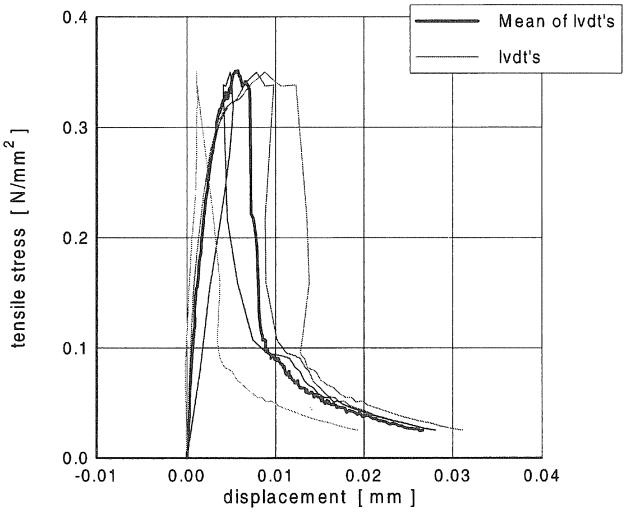

Fig. 13. Example of differences between mean displacement and the displacements of the corners in a tensile test from the WC-JO+1:1:6 series

Net bond area

During the first series in 1990, it became clear by close observation of the cracked specimens, that the area where the mortar-joint and unit were bonded together, was smaller than the cross-sectional area of the specimen. For each of the masonry specimens in that series the "net bond surface" was determined by visual inspection of the crack-surface. An example is shown in Figure 14. Taking the net bond surface into account, reduces the coefficients of variation of the tensile bond strength and the fracture energy with respectively 34% and 18%.

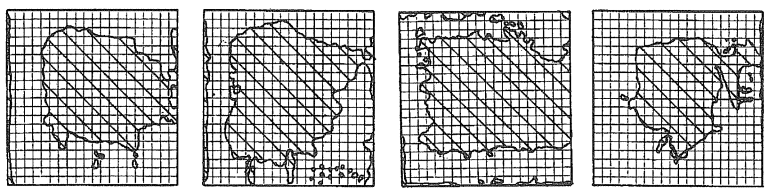

Fig. 14. Net bond surface of SM-VE masonry specimens with 1:2:9 mortar.

In many cases the net bond surface was restricted to the central part of the specimen. Therefore it is supposed that the reduction of the bond surface is caused by the edges of the specimen. This may be the result of setting of the mortar in its plastic phase and of shrinking. In a normal wall, two of the four edges are not present. With the proposed influence of the edges, it is possible to estimate the fracture energy for a wall (see Figure 15). The average bond surface of the specimens was 35% of the cross-sectional area. If the net bond surface is supposed to be square, it follows that the net bond surface of a wall will be 57% of the cross-sectional area. So the bond surface of the wall is approximately 1.7 times greater than that of the specimens. The same holds true for the fracture energy and the tensile strength of the wall; both based on the gross cross-sectional area. It is noted that a possible influence of perpends is totally neglected in this way.

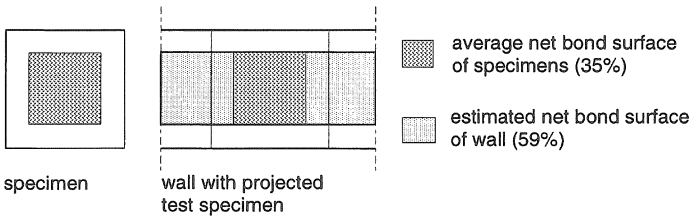

Fig. 15. Estimation of the net bonding surface of a wall based on the average net bonding surface of the tests specimens.

4 Flexural Tests

4.1 Testing Arrangement

A 4-point bending test arrangement was used. With this testing arrangement G_{fl} can be established, but it is not possible to establish the stress-crack width relation. The deflection of the specimen measured on the specimen itself, was used as the control parameter. Using this parameter it was possible to continue the test after the maximum load has been reached and consequently G_{fl} could be established. The test set-up is presented in Figure 16 in detail.
This testing arrangement was used, because it was expected that specimen types that failed in the tensile test set-up, could be controlled more easily. Although controlling the tests was difficult (very steep descending branches), it was possible to establish values for the fracture energy of CS-brick masonry with 1:1:6 mortar: something that was not achieved in the series of 1990 and 1993.

LVDT a in Figure 16 was used to control the deformation. The maximum deflection that could be measured with this LVDT was 0.4 mm. All bearings were hardened steel roller bearings to avoid friction.

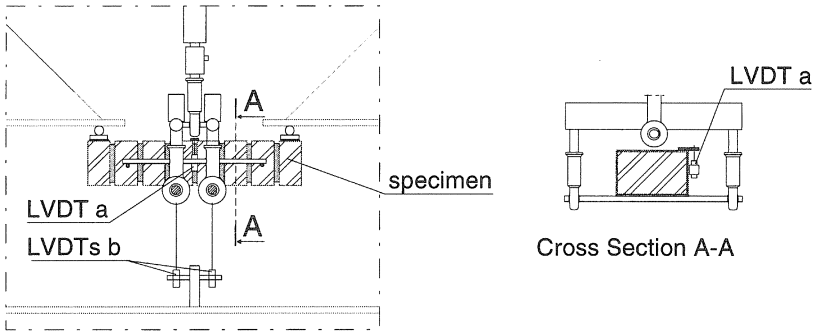

Fig. 16. Detailed view of a specimen in the 4-point bending test arrangement.

It can be observed that the deflection used to control the test, was only measured over a part of the span. Using the deflection over the whole span lead to uncontrolled failure. LVDTs b were used to measure the distance covered by the load. The maximum displacement that could be measured with these LVDTs was 2 mm. Although nearly the same measurement could be performed with the internal LVDT of the actuator, LVDTs b were used because of their more accurate measurements. In some tests their signals were suddenly out of their measuring range, probably caused by small physical disturbances. In these cases the internal LVDT of the actuator was used to establish the amount of work added to the specimen. The reliability of those results is discussed in section 4.3.

4.2 *Specimens*

The specimens used for the flexural test are presented in Figure 17. The exact dimensions of the stack bonded prism depended on the brick type used. All stack bonded prisms were 6 bricks high.

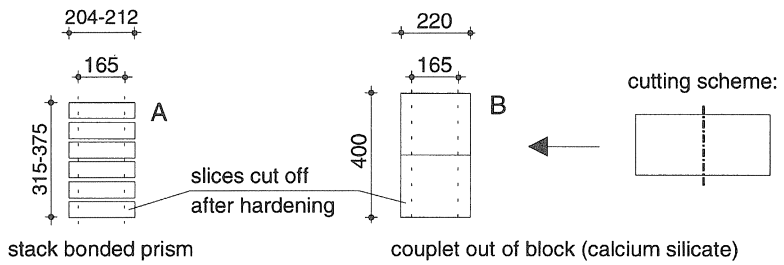

Fig. 17. Flexural Specimens.

After hardening slices were cut off the specimens to adjust their width to the testing arrangement.

4.3 *Results and discussion*

In Figure 18 an example of the measured data in a test is presented.

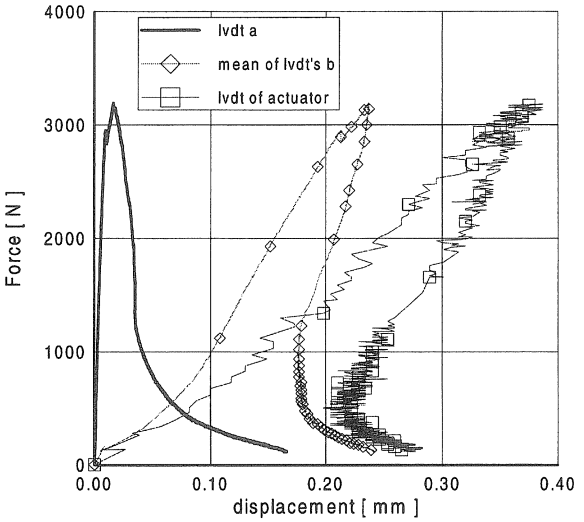

Fig. 18. Example of measured date in the flexural test.

It can be seen that LVDT a always gave an increasing deformation whereas the displacement measured with LVDTs b and the internal LVDT of the actuator showed snap back behaviour. Uncontrolled failure would be the result, if the last two signals would have been used to control the increase of deformation. It can also be observed that the area under the diagram of LVDTs b and the internal LVDT of the actuator are approximately the same. These area's are equal to the amount of work done.

The flexural bond strength f_{fl} was calculated from:

$$f_{fl} = \frac{M_u}{W}$$

in which:

M_u is the ultimate bending moment in the mortar-joint that failed;

W is the elastic section modulus.

This way of calculating the flexural strength assumes a fictitious linear stress distribution at failure. The non-linear stress distribution in the cross section at ultimate load is presented in Figure 19 with the bold solid line.

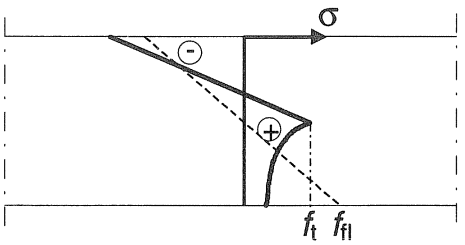

Fig. 19. Non-linear stress distribution (solid line) due to bending and the fictitious elastic distribution (dashed line) at the maximum load level.

The results of all tests are presented in tables in the annex. In each table, test results for one type of unit are presented.
In Table 6 the mean test results for all material combination are presented, including the CV between brackets.

Table 6. Average results of flexural tests.

test series	specimen type	mortar	f_{fe} [N/mm^2]	G_{fl} [N/mm]	$G_{fl;cyl}$ [N/m]
1995	sm-RIJ	1:1:6	0.19 (37%)	0.0091 (41%)	8.7 (65%)
	wc-JO	1:1:6	0.58 (34%)	0.0120 (102%)	11.7 (77%)
	CS-brick	1:1:6	0.23 (41%)	0.0038 (52%)	4.2 (48%)
	CS-block	tlm	0.39 (35%)	0.0070 (52%)	7.5 (47%)

The differences between the means of both ways of determining the fracture energy (G_{fl} by means of LVDT a and $G_{fl;cyl}$ by means of the internal LVDT of the actuator), are not significant so it may be concluded that the use of the data from the internal LVDT of the jack worked satisfactory. However, when the results for individual specimens are observed separately (see Table 12 - Table 15) both methods can give very different results.
The flexural strength of the masonry with the sm-RIJ is relatively low, but this result is of the same magnitude as results of sm-VE clay brick masonry. When the flexural strength of the series with wc-JO clay bricks with 1:1:6 mortar and CS-blocks with thin layer mortar is compared with the corresponding tensile bond strength presented in Table 4 on page 12, it can be observed that the flexural strength is 1.5 respectively 1.2 times greater. These differences can be explained with the non-linear stress distribution in a bending test at failure as presented in Figure 19 (Van der Pluijm, 1995).

5 Comparison between the fracture energy determined in the tensile and the flexural testing arrangement

The fracture energy of masonry consisting of wire cut JO clay bricks with 1:1:6 mortar and of CS-blocks with thin layer mortar determined in the tensile and flexural tests can be compared, because the specimens for both test arrangements were made simultaneously with the same mortar batches. It can be observed that the fracture energy determined with the flexural tests is 2 to 3 times higher than that determined with the tensile tests. This difference can partly be explained with the shape of the bonding surface. As we have seen, a ratio = 1.7 can be expected between the values of couplets and walls. This ratio was based on the observed bonding area in the small masonry specimens C of Figure 5. A schematic view was presented in Figure 15.
From the bonding surface of the failed flexural specimens, it could be observed that this phenomenon played a role. Because two slices on the head sides of the flexural specimens were cut off, the bonding surface of the clay brick flexural specimens was practically the same as that suggested for a wall in Figure 15. An example is shown in Figure 20.

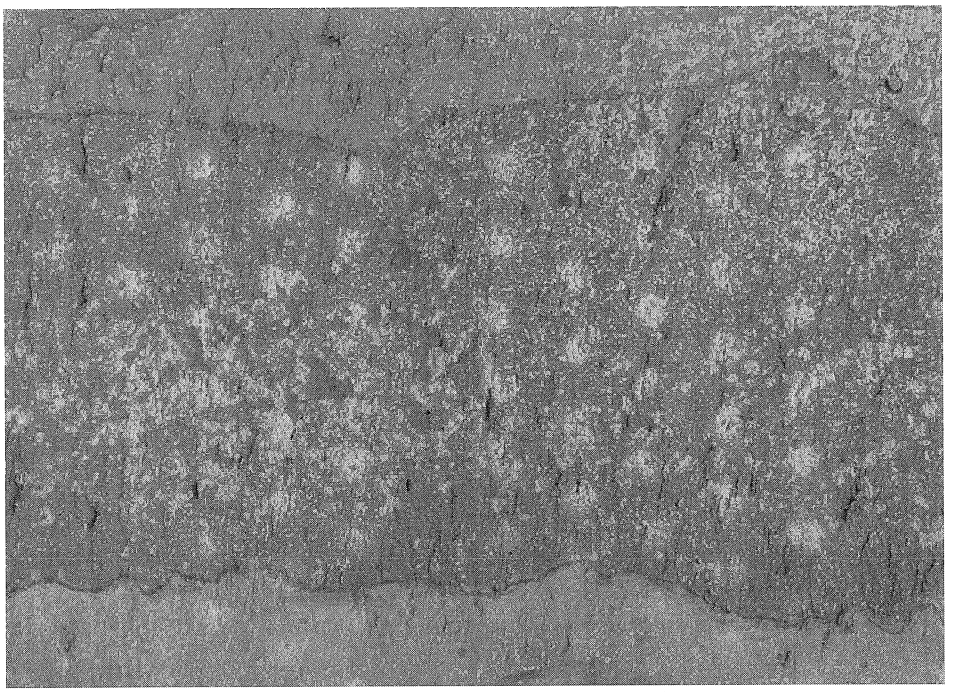

Fig. 20. Example of the bonding surface of a cross section of a soft mud clay brick specimen after failure (the dark area in the middle corresponds with the actual bonding surface).

Although this phenomenon could also be observed for the bonding surfaces of calcium silicate specimens, it was less obvious there.

Hordijk (1992) has found another explanation for the difference that can occur between flexural and tensile tests on plain concrete. He found that the crack width in the middle of the specimens at the end of the tail of the flexural tests was larger than in the tensile tests and that the determination of G_{fl} is sensitive for the length of the tail. Hordijk considered the average maximum deformation in cracks of his tensile tests as the upper limit for the crack width in the middle of the flexural specimen when the amount of work is calculated. Doing this, he found a remarkable agreement between tensile and flexural tests. Analysing the tests here in the same way, showed that the mean crack width in the bending tests at the end of the force-crack width diagram was somewhat greater than the average crack width at the end of a tensile test. However, taking this difference into account hardly changed the values found for the fracture energy.
Another explanation for the difference is as follows. As we have seen in Figure 13, a specimen in the tensile test set-up is more or less free to choose where in the cross section the crack starts to occur and to follow the unloading path with the least "resistance".
In the flexural tests this is not the case: the crack must start to develop at the bottom of the specimen and is forced to the top of the specimen while the neutral axis is kept horizontal. The irregular shaped area where bonding has occurred will probably contribute to this phenomenon.

6 Concluding Remarks

With the presented test results and formulations for the descending branches, it is possible to model the behaviour of masonry under tension in a non-linear way on a meso-level. When this kind of data is used in numerical finite element models, it is strongly advised that the sensitivity of calculation results for the variation of the fracture energy and bond strength is established because of the "natural" large scatter of bond properties of masonry.

7 Acknowledgements

The experiments described in this paper, were carried out as a part of a national masonry research program financed by the Dutch masonry industries and the government and as a part of a thesis study financed by the Technology Foundation (STW) under grant EBW 44.3367.

8 References

HORDIJK, D.A, (1992), *Tensile and tensile fatigue behaviour of concrete; experiments modelling and analyses*, HERON Vol. 37 no. 1, 79 pp.

LOURENÇO, P.B; J.G. ROTS, J. BLAUWENDRAAD (1995), *Two approaches for the analysis of masonry structures: micro- and macro-modelling*, HERON, Vol. 40 No. 4, pp. 313-340.

PETERSSON, P.E. (1981), *Crack growth and development of fracture zones in plain concrete and similar materials*, Report TVBM-1007, Lund Institute of Technology, Sweden, 174 pp.

VAN DER PLUIJM , R, VERMELTFOORT, A.TH. (1991), *Deformation Controlled Tensile and Compression Tests on Units, Mortar and Masonry*, TNO-report B-91-0561 (in Dutch).

VAN DER PLUIJM, R. (1992), *Material Properties of Masonry and its Components under Tension and Shear*, Proceedings of the 6th Canadian Masonry Symposium, Saskatoon, Canada, pp. 675-686.

VAN DER PLUIJM, R. (1993), *Shear Behaviour of Bed Joints*, Proceedings of the Sixth North American Masonry Conference (Ed. D.P. Abrams), Philadelphia, 6-9 June, pp.125-136.

VAN DER PLUIJM, R (1995), *Numerical Evaluation of Bond Tests*, Masonry International, Vol. 9, No. 1, pp. 16-25, issn 0950-2289

VAN MIER, J.G.M. A. VERVUURT, E. SLANGEN, 1994, *Boundary and Size Effects in Uniaxial Tensile Tests: A Numerical and Experimental Study*, Fracture and Damage in Quasibrittle Structures, Eds Z.P. Bazant, Z. et al., E&FN, ISBN 0 419 19280 8

VEKEY, R.C. DE; PAGE, A.W; HEDSTROM, E.G., 1994, *The Variability of Bond Wrench Measurements in UK, Australia and USA*, Masonry International, Vol. 8 No. 1 pp. 21-25.

VERMELTFOORT, A.TH, VAN DER PLUIJM, R. (1995), *Bond Wrench Testing*, Proceedings of the British Masonry Society, Masonry (7), Proceedings of the 4th International Masonry Conference, London, 23-25 October, 1995, pp.225-231.

Annex

In each table, test results for one type of test and one type of unit are presented. Within a table the results are grouped by mortar batch. For each brick-mortar combination the average value is given with the coefficient of variation between brackets.
The following abbreviations and special characters are used in the tables:

*	uncontrolled test beyond the top;
-	not applicable or not calculated;
tlm	thin layer mortar;
fmgpm	factory made general purpose mortar;
CV	coefficient of variation.

Tensile tests

Table 7. Tensile tests with soft mud Vijf Eiken clay bricks (sm-VE) (specimens are grouped by specimen type or different mortar batches).

test series	specimen type (see Figure 5)	mortar	E_o^j [N/mm²]	E_u^j [N/mm²]	G_{fl} [N/m]	f_t [N/mm²]
1990	prism A	-	-	-	52	2.24
			-	-	78	2.88
			-	-	54	2.29
	average (CV)				61 (24%)	2.47 (14%)
	cylinder B	-	-	-	71	1.44
			-	-	72	1.57
			-	-	75	1.50
	average (CV)				73 (3%)	1.50 (4%)
	masonry prism C	1:2:9	730	360	3.7	0.14
			950	501	10.4	0.37
			670	345	13.5	0.35
			520	320	*	0.07
			640	408	3.4	0.18
	average (CV)		700 (22%) *	390 (18%)	7.8 (65%)	0.22 (60%)
	masonry prism C	1:½:4½	670	179	3.4	0.07
			990	351	5.7	0.28
			190	52	3.4	0.04
	average (CV)		620 (65%) **	194 (77%)	4.2 (32%)	0.13 (101%)

*) determined with lin. regression between 0 and 0.50 f_t for an optimal correlation coefficient ($r > 0.99$)
**) determined with lin. regression between 0 and 0.63 f_t for an optimal correlation coefficient ($r > 0.99$)

Table 8. Tensile tests with wire cut Joosten clay bricks (wc-JO) (specimens are grouped by specimen type or different mortar batches).

test series	specimen type (see Figure 5)	mortar	E_o^j [N/mm²]	E_u^j [N/mm²]	G_{fI} [N/m]	f_t [N/mm²]
1990	prism A	-	- -	- -	- 117	2.01 2.72
	average (cv)				117 (-)	2.36 (21%)
	cylinder B	-	- - -	- - -	129 131 124	3.48 3.43 3.61
	average (cv)				128 (3%)	3.51 (3%)
	masonry prism C	1:2:9	2532 2887 3266	592 1635 2012	9.8 19.6 5.2	0.24 0.38 0.28
	average (cv)		2895 (13%) *	1413 (52%)	11.5 (64%)	0.30 (24%)
	masonry prism C	1:½:4½	5269 6165 4384	2316 2994 6229	8.1 10.8 3.2	0.40 0.52 0.41
		1:½:4½	5826 8049 6316	3829 4686 2959	5.3 10.4 3.0	0.43 0.77 0.44
	average (cv)		6002 (20%) **	3836 (37%)	6.8 (51%)	0.50 (29%)
1995	masonry prism C	1:1:6	3493 2815 2143 2139	1905 728 1533 1224	3.3 1.7 1.9 3.7	0.52 0.27 0.28 0.37
		1:1:6	1942 632 1436 2193 1699 1145	822 541 644 758 546 607	9.1 6.8 3.1 * 11.2 9.6	0.44 0.36 0.35 0.64 0.39 0.49
		1:1:6	1568 1207 2717 706 1329 1052	1305 643 908 305 1096 734	2.2 1.8 3.4 * 3.2 2.3	0.25 0.24 0.43 0.08 0.45 0.22
		1:1:6	2630 1868 2179 3121 2711	1486 923 960 2126 1742	4.1 3.2 2.4 * 6.2	0.38 0.3 0.31 0.57 0.49
		1:1:6	3811 3192 5528 1761 560 1564	2464 2718 3229 830 617 492	9.1 * * * 1.4 6.9	0.44 0.44 0.81 0.37 0.14 0.3
		1:1:6	2272 4202 1519 4273 1622 5986	906 1417 773 1446 1127 1832	13.6 8.5 2.6 8.2 3.7 14.8	0.69 0.56 0.32 0.53 0.23 0.57
	average (cv)		2371 (55%) ***	1216 (57%)	5.5 (70%)	0.40 (39%)

* determined with lin. Regression between 0 and 0.57f_t for an optimal correlation coefficient (r > 0.99)
** determined with lin. Regression between 0 and 0.52f_t for an optimal correlation coefficient (r > 0.99)
*** determined with lin. Regression between 0 and 0.69f_t for an optimal correlation coefficient (r > 0.98)

Table 9. Tensile tests with Calcium Silicate bricks, blocks and elements (CS) (specimens are grouped by specimen type or different mortar batches).

test series	specimen type (see Figure 5)	mortar	E_o^j [N/mm²]	E_u^j [N/mm²]	G_{fI} [N/m]	f_t [N/mm²]
1990 bricks	unit prism A	-	- - -	- - -	71 74 56	2.11 2.36 2.56
	average (CV)				67 (17%)	2.34 (10%)
	masonry prism C	1:2:9	4286 4907 4884 6360	1274 1708 1420 1561	* * * *	0.31 0.22 0.47 0.27
	average (CV)		5109 (17%) *)	1491 (12%)		0.32 (34%)
	masonry prism C	1:1:6	2289 3299 2659 2020 2414	1389 2231 1983 1652 1668	* * * * *	0.18 0.46 0.30 0.17 0.55
	average (CV)		2536 (19%) **)	1785 (18%)		0.33 (51%)
1993	unit prism A (out of element 900 × 100 × 600 mm)	-	- - - -	- - - -	* * 47 *	1.13 0.69 1.99 0.85
	average (CV)				47 (-)	1.17(49%)
1995 blocks			E_o^{j+u} ****	E_u^{j+u} ****		
	masonry prism D	tlm	3874 5840 4242 8297 9433 5036 10827 2782 9911 5459 3793	3045 4902 2689 8209 10170 3876 4443 1528 5531 3428 2820	* * * * * 2.0 * 1.6 5.1 * *	0.35 0.31 0.21 0.29 0.34 0.35 0.35 0.18 0.38 0.38 0.15
		tlm	4737 5908 4256 7644 3718 3217 13171 5091 8314 4871	3835 5097 2795 6004 2689 2121 9386 4152 7691 2985	* * * * * * * 3.4 * *	0.45 0.28 0.16 0.31 0.29 0.21 0.32 0.28 0.42 0.37
		tlm	8233 6573 5814 11906 16582 11312 8321 7469 12372 20154 11507 12988	5947 6037 3676 9712 10519 9815 4122 6736 12995 11616 9804 11076	* 5.6 2.0 * 2.6 3.0 * 3.1 * * 4.3 *	0.44 0.36 0.25 0.25 0.35 0.36 0.40 0.44 0.48 0.43 0.51 0.37
	average (CV)		7989 (54%) ***)	6044 (53%)	3.3 (41%)	0.33 (27%)

* determined with lin. regression between 0 and 0.50 f_t for an optimal correlation coefficient ($r > 0.99$)
** determined with lin. regression between 0 and 0.54 f_t for an optimal correlation coefficient ($r > 0.99$)
*** determined with lin. regression between 0 and 0.82 f_t for an optimal correlation coefficient ($r > 0.92$)
**** no reliable values could be obtained for single mortar-joints ($r \approx 0.77$), therefore results over the gauge length (35 mm) are presented

Table 10. Tensile tests with high strength wire cut Joosten Kessel clay bricks (hswc-JOK).

test series	specimen type (see Figure 5)	mortar	E_o^j [N/mm^2]	E_u^j [N/mm^2]	G_{fl} [N/m]	f_t [N/mm^2]
1993	prism 47 × 47 × 102	tlm	4455	2830	13.4	2.56
	prism 48 × 45 × 102		3354	2484	26.0	1.84
	prism 96 × 100 × 102		4612	1857	*	1.57
	cylinder ø50 × 102		5264	4561	16.0	3.06
	cylinder ø50 × 102		4326	3971	13.1	2.18
	average (CV)		4402 (16%)*	3141 (35%)	17.1 (32%)	2.24 (26%)

* determined with lin. regression between 0 and 0.85 f_t for an optimal correlation coefficient ($r > 0.94$)

Table 11. Tensile tests with normal density concrete bricks (MBI).

test series	specimen type (see Figure 5)	mortar	E_o^j [N/mm^2]	E_u^j [N/mm^2]	G_{fl} [N/m]	f_t [N/mm^2]
1993	masonry prism C	fmgpm	8133	6219	*	0.82
			9616	9168	11.3	0.50
			9532	10917	*	0.84
			4497	4222	*	0.76
			8430	6838	*	0.73
	average (CV)		8042 (26%)*	7473 (35%)	11.3 (-)	0.73 (19%)

* determined with lin. regression between 0 and 0.93f_t for an optimal correlation coefficient ($r > 0.92$)

Flexural tests

Table 12. Flexural tests with soft mud clay bricks Rijswaard (sm-RIJ).

test series	specimen type (see Figure 17)	mortar	f_{fl} [N/mm^2]	G_{fl} [N/m]	$G_{fl;cyl}$ [N/m]
1995	stack bonded prism A	1:1:6	0.25	9.2	8.1
			0.26	*	*
			0.12	6.5	4.7
			0.19	11.7	12.7
	average (CV)		0.19 (37%)	9.1 (41%)	8.7 (65%)

Table 13. Flexural tests with wired cut clay bricks Joosten (wc-JO) (specimens are grouped by mortar batch)

test series	specimen type (see Figure 17)	mortar	f_{fl} [N/mm^2]	G_{fl} [N/m]	$G_{fl;cyl}$ [N/m]
1995	stack bonded prism A	1:1:6	0.42	2.4	4.9
			0.72	-	5.2
		1:1:6	0.90	-	29.6
			0.34	4.0	4.7
		1:1:6	0.39	3.4	3.2
			0.39	4.4	7.3
			0.53	7.5	5.6
			0.36	-	4.5
		1:1:6	0.55	3.6	7.8
			0.40	4.2	7.3
			0.61	8.6	10.5
		1:1:6	0.50	-	18.0
			0.84	8.2	14.7
			0.65	19.3	4.3
		1:1:6	0.71	15.3	16.9
			1.00	36.8	24.9
			0.64	38.0	28.9
	average (CV)		0.58 (34%)	12.0 (102%)	11.7 (77%)

Table 14. Flexural tests with Calcium Silicate bricks and blocks (CS-brick / CS-block) (specimens are grouped by specimen type and mortar batch).

test series	specimen type (see Figure 17)	mortar	f_{fl} [N/mm^2]	G_{fl} [N/m]	$G_{fl;cyl}$ [N/m]
1995	couplet C (blocks)	tlm	0.21	10.3	2.8
			0.59	-	13.6
			0.22	4.2	6.3
		tlm	0.35	7.1	5.0
		tlm	0.48	3.7	10.0
			0.45	11.0	11.8
			0.28	-	6.1
			0.39	5.4	5.2
			0.54	7.1	6.5
	average (cv)		0.39 (35%)	7.0 (52%)	7.5 (47%)
	stack bonded prism A (bricks)	1:1:6	0.25	*	*
			0.16	2.4	2.8
			0.27	*	*
			0.35	5.1	5.6
			0.11	*	*
	average (cv)		0.23 (41%)	3.8 (52%)	4.2 (48%)

Table 15. Flexural tests with normal density concrete bricks (MBI) (specimens are grouped by specimen type).

test series	specimen type (see Figure 17)	mortar	f_{fl} [N/mm^2]	G_{fl} [N/m]	$G_{fl;cyl}$ [N/m]
1995	stack bonded prism A	fmgpm.	0.52	14.5	14.5
			0.41	8.6	8.5
			0.51	19.4	16.4
			0.35	9.2	9.2
			0.50	4.2	6.7
	average (CV)		0.46 (16%)	11.2 (52%)	11.1 (38%)
	stack bonded prism C	tlm	0.84	24.8	26.7
			1.50	39.5	40.5
			1.29	44.8	45.9
			1.20	43.4	45.1
			1.40	*	*
			1.34	45.8	47.7
	average (CV)		1.26 (18%)	39.6 (22%)	41.2 (21%)